



CHORUS

This is the accepted manuscript made available via CHORUS. The article has been published as:

Charge transport in DNA nanowires connected to carbon nanotubes

Bikan Tan, Miroslav Hodak, Wenchang Lu, and J. Bernholc

Phys. Rev. B **92**, 075429 — Published 19 August 2015

DOI: [10.1103/PhysRevB.92.075429](https://doi.org/10.1103/PhysRevB.92.075429)

Charge Transport in DNA Nanowires

Bikan Tan, Miroslav Hodak, Wenchang Lu, and J. Bernholc

Center for High Performance Simulation and Department of Physics,

North Carolina State University, Raleigh, NC 27695-7518

(Dated: August 5, 2015)

Abstract

DNA is perhaps the world's most controllable nanowire, with potential applications in nanoelectronics and sensing. However, understanding of its charge transport (CT) properties remains elusive with experiments reporting a wide range of behaviors from insulating to superconductive. We report extensive first-principle simulations that account for DNA's high flexibility and its native solvent environment. The results show that the CT along the DNA's long axis is strongly dependent on DNA's instantaneous conformation varying over many orders of magnitude. In high CT conformations, delocalized conductive states extending over up to 10 base pairs are found. Their low exponential decay constants further indicate that coherent CT, which is assumed to be active only over 2-3 base pairs in the commonly accepted DNA CT models, can act over much longer length scales. We also identify a simple geometrical rule that predicts CT properties of a given conformation with high accuracy. The effect of mismatched base pairs is also considered: while they decrease conductivities of specific DNA conformations, thermally-induced conformational fluctuations wash out this effect. Overall, our results indicate that an immobilized partially dried poly(G)-poly(C) B-DNA is preferable for nanowire applications.

I. INTRODUCTION

DNA is a remarkable molecule: in addition to being a blueprint for life its properties also make it attractive for use in several fields of technology. One of them is molecular electronics, where its one-dimensional character and the ease with which it can be synthesized in a precisely determined sequence make it a potential candidate for nanowires and other applications. However, DNA's conductive properties remain disputed. The idea that DNA can conduct current along its long axis was first proposed in 1962,¹ but subsequent studies found behaviors spanning a tremendous range: insulating,^{2,3} semiconducting,⁴ metallic⁵ and even superconducting.⁶ Potential reasons for this spread is DNA's high sensitivity to factors such as its length, sequence, environment (solvent, counterions, impurities, etc.), and contacts. In addition, unlike other candidates for nanowires, DNA is highly flexible at room temperature, with molecular vibrations an order of magnitude larger than in crystals.⁷ This enables easy unzipping of the DNA duplex, which is important for DNA's biological role, but it complicates computational modeling and interpretation of experimental results.

Experiments that utilized well-defined DNA contacts and preserved the native conformation achieved more consistent results, measuring conductivities between $10^{-5}G_0$ and $10^{-2}G_0$,⁸⁻¹³ where $G_0 = 2e^2/h = 12.9 k\Omega$ is the fundamental unit of ballistic conductance. In particular, Guo *et al.*¹³ used a setup with a 15 base pair (bp) DNA connected to carbon nanotube leads and ensured that only a single molecule bridged the leads. This work found a consistent conductivity and observed that a single mismatched pair causes a large drop in the current.

Similarly to other molecular wires,¹⁴ charge transport (CT) in DNA is commonly explained in terms of two processes: superexchange and hopping. The former is a coherent process in which a hole tunnels directly from a donor to an acceptor without occupying the intervening base pairs. It is assumed to only act over distances of a few base pairs. Long distance CT, which has been reported for distances of over 200 Å,^{9,15} is commonly explained in terms of hopping. That is a multi-step mechanism, in which holes migrate through the DNA by hopping between either guanines or adenines sites^{16,17} with each individual step accomplished by a superexchange process. Coherent transport over delocalized states can also contribute as evidenced by experimental findings of delocalization of wavefunctions for holes,¹⁸⁻²⁷ but their extent has been estimated to be 3 base pairs or less.^{23,28-31} While one

experiment³² indicated that a single-step coherent transport over delocalized states spanning over the entire molecule is the dominant mechanism for distances of over 10 base pairs, other studies continue to find much shorter extent of coherent transport.^{33,34}

Another controversial topic is identification of factors controlling DNA conductivity. DNA is highly flexible at room temperature, with molecular vibrations as large as a tenth of the lattice constant, meaning that the DNA duplex is on the verge of melting.^{7,35} Furthermore, the surrounding water molecules and ions also evolve dynamically. Studies investigating the relative importance of these factors have come to differing conclusions. Barnett et al.³⁶ proposed a gating role for positive ions, while others^{29,37,38} posited a critical role of water molecules causing localization of conducting states. Finally, Barton and coworkers introduced a concept of conformational gating,^{23,39} in which the DNA conformation plays a critical role and only certain thermally excited DNA conformations are CT-active while others do not contribute to the CT.

Computer simulations can provide important insight into CT in DNA, but DNA's length, high flexibility and sensitivity to the environment make computational studies challenging. Consequently, only a handful of fully quantum CT studies exist in the literature, despite the fact that CT is an inherently quantum phenomenon. The existing works have been limited to a single conformation to keep the computational cost manageable, thus ignoring the effects of molecular vibrations. One of the studies investigated a dry 6 bp (base pair) poly(G)-poly(C) A-DNA connected to gold leads and found that conductance values range from $10^{-13}G_0$ to $10^{-16}G_0$.⁴⁰ It also concluded that the observed CT is due to a sequence-specific short-range tunneling across a few bases combined with general diffusive/inelastic processes. A different work⁴¹ studied a 4 bp poly(G)-poly(C) B-DNA snapshot connected to gold leads. It considered both dry and hydrated cases and found that hydration enhances the current by an order of magnitude at the gate bias of 0.3 V. Ref. 42 investigated sequence dependence of electron transport in wet DNA. The calculation used a configuration averaged from 10 snapshots sampled over a 1 ns MM simulation. They found that GC domains, where delocalized orbitals are located, are necessary for efficient conductance through DNA. Qi et al.⁴³ investigated conductance of four different strands of dry ideal 15 bp B-DNA. Comparison to the experiment⁴⁴ showed a large discrepancy, which was substantially improved by adding decoherence of appropriately chosen strength.

Here, we report fully quantum charge transport calculations, which sample multiple room

temperature conformations, account for solvent and use a realistic setup that mirrors the experiment.¹³ Our results show dramatic changes in the current depending on DNA’s instantaneous configuration. For high CT conformations, delocalized domains spanning the entire length of 10 bp DNA are found. A weak distance dependence further indicates that the coherent transport can act over far longer distances than commonly assumed. We also find that the complicated structure/CT relationship can be expressed in terms of a single structural parameter.

II. METHODOLOGY

The setup of quantum transport calculations is based on experiment by Guo *et al.*,¹³ who connected a partially dried 15 bp double-stranded B-DNA to carbon nanotube leads via alkane linkers $CONH - (CH_2)_3$. We use the same linker with (5,5) nanotubes and either 10 or 4 bp-long double-stranded B-DNA. The shorter DNA is used to make many quantum transport calculations computationally tractable. The first solvation shell, i.e., the solvent and ions within 3 Å from DNA, is included in transport calculations. The solvent further is neglected because (i) the current is efficiently screened by the first layer, and (ii) the wave functions of DNA are compact and thus are only affected by the nearby solvent. Therefore, the calculated quantum transmission is thus a good representation of transmission in fully solvated DNA. The setup of the transport calculations is displayed in Fig. 1(a).

Because DNA is highly flexible at room temperature, we sample several of its conformations at room temperature, rather than the ideal B-DNA structure. The conformations are obtained from molecular mechanics (MM) calculations, which consider a fully solvated DNA connected to nanotubes via alkane linkers as described above. The calculations use NAMD⁴⁵ with CHARMM27⁴⁶ force field. As is the case in solvated DNA, phosphate groups in DNA backbone are deprotonated and Na^+ ions are added to balance the charge of the system. In addition, Na^+ and Cl^- ions are added to the solution to achieve concentration of 0.05 mol/L. A total of up to 78,000 atoms are included in MM calculations. The systems are initially equilibrated for 0.5 ns, after which runs are continued for additional 2 ns, during which 20 snapshots are recorded. When investigating CT of a given DNA conformation, 5 snapshots are extracted from a 1 ns MM calculation with DNA kept frozen, to account for changes caused by the dynamics of the solvent environment.

The recorded snapshots are analyzed at the quantum level using the non-equilibrium Green function (NEGF) technique^{47–49} as implemented in our real-space multigrid (RMG) code.^{50–53} These calculations include solvent and counter ions within 3 Å from DNA surface for a total of up to 1,800 atoms. The total charge of the omitted counter ions is included as a uniform charged background. In the localized orbital quantum calculations, six orbitals per atom with a cutoff radius of 9 Bohr are used. The electron-ion interactions are represented by ultrasoft pseudopotentials.^{54,55} Generalized gradient approximation in the PBE form⁵⁶ is used for the exchange and correlation terms. The potential and charge density of the leads are fixed to those corresponding to the bulk material. The effects of the infinite CNTs are included in the self-energy terms of the left (L) and right (R) leads. Eight atomic layers of CNT are included at both sides of the central conductor (C) to account for screening effects, so that the potential and the charge density match at the interfaces between the conductor and the leads after self-consistent calculations. The Hartree potential is obtained by solving Poisson equation with the boundary condition of matching the potential of all the leads. After the KS potential and the charge density are obtained self-consistently, we calculate the transmission coefficient using the Landauer formula:

$$T(E) = Tr[\Gamma_L(E)G_C^R(E)\Gamma_R(E)G_C^A(E)] \quad (1)$$

Here Γ_L, Γ_R and G_C^R, G_C^A are the coupling functions for the left and right leads and the retarded and advanced Green's functions of the conductor part, respectively. The current is obtained by integrating the transmission curve over the HOMO band below the Fermi level using a source-drain bias of $V_{sd} = 50mV$:¹³

$$I = \frac{2e^2}{h} \int_{-V_{sd}}^0 T(E)dE. \quad (2)$$

The 3DNA code⁵⁷ was used to build and analyze DNA structures and PyMOL⁵⁸ was used for structural visualization.

III. RESULTS AND DISCUSSION

The atomic configuration of a 10 bp poly(G)-poly(C) B-DNA fragment is shown in Fig. 1(b), and the results of quantum-transport calculations for 20 room temperature snapshots extracted from a MM simulation of this system are shown in Fig. 1(c). The current varies

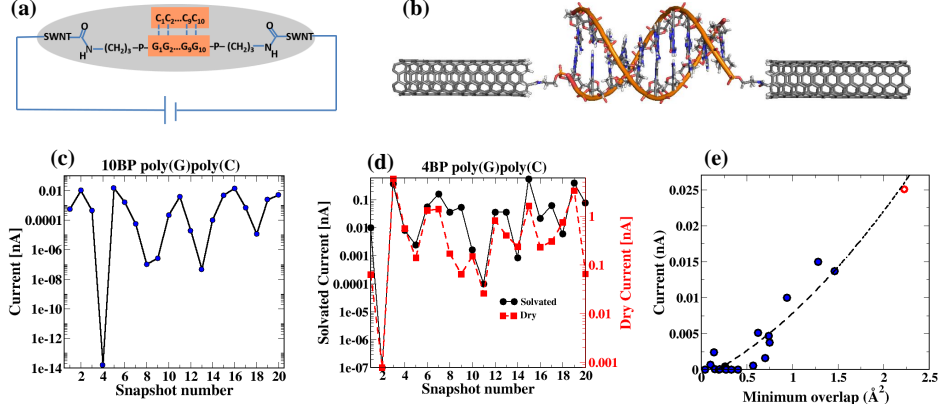


FIG. 1. (a) Schematic of the simulated DNA conductivity measurement setup. The shaded area represents explicit solvation. (b) The atomic configuration of the 10 bp poly(G)-poly(C) B-DNA attached to nanotube leads. Water and counterions are omitted for clarity. (c) Currents for 20 room temperature snapshots of 10 bp poly(G)-poly(C) B-DNA in the above configuration. (d) Currents for 20 room temperature snapshots of dry and solvated 4-bp poly(G)-poly(C) DNA. The y-scale is different for each case and is chosen so that the minima and maxima lie on the bottom and the top of the figure, respectively. (e) Conductivity of 10 bp poly(G)-poly(C) DNA snapshots vs. minimum of overlap areas between guanines. The empty circle is for the canonical B-DNA. The dashed line is a quadratic fit to the data.

over many orders of magnitude between the snapshots, from a maximum of 0.015 nA to a minimum of $1.6 \cdot 10^{-14}$ nA, the average being 0.003 nA. The differences are due to changes in delocalization of the conductive HOMO states located mainly on guanines: while they extend over the entire molecule for the most conductive conformations, they are much more localized in the less conductive configurations. This is visualized in Figs. 2 (a) and (b) for two examples: a highly conductive configuration and a highly resistive one.

The finding that conductive states can extend over a substantial distance shows that coherent transport certainly contributes to long-range CT in DNA, in agreement with recent experimental results.³² However, several studies have argued that ions^{29,36–38} and water molecules^{23,29,37} surrounding DNA have localizing effects on the conductive states, thus greatly limiting their extent. Nevertheless, our results demonstrate that for the right configurations of DNA and its surrounding environment, extended conducting orbitals, delocalized over at least 10 bp — or 1 full B-DNA turn — can exist.

To separate the effect of DNA conformation from that of its environment, CT in dry and solvated DNA is compared. For computational efficiency, this is done on a shorter 4 bp poly(G)-poly(C) DNA. The currents of 20 investigated snapshots are shown in Fig. 1(d). Solvation and counterions suppresses the average current by about an order of magnitude but, importantly, they do not change the overall trend with the low and high conductive snapshots remaining such, regardless of solvation. Therefore, we conclude that the main parameter determining conductivity of DNA is its conformation. Several studies have proposed gating roles for either water or ions^{29,36-38} but our results show that the effects of conformation are much stronger. The finding that DNA conformation determines which configurations are conductive and which are not confirms the concept of conformational gating introduced by Barton and coworkers, who proposed that only certain DNA conformations are CT-active.^{23,39}

To investigate which structural properties of DNA are critical for CT, we calculate correlations between currents of the 10 bp poly(G)-poly(C) B-DNA room temperature snapshots and standard DNA-structure parameters. The following single and two-base-pairs parameters, as implemented within 3DNA,⁵⁷ are considered: shear, stretch, stagger, buckle, propeller, opening, shift, slide rise, tilt, role, twist, x-displacement, y-displacement, inclination, tip, and overlap area. For each of these we consider its average, minimum and maximum over the entire length of the DNA. The correlation coefficients for the inter base pair parameters are given in Table I. We find that only the minimum of overlap areas between guanines shows a significant correlation with the current, with correlation coefficient being more than 0.9. This can be intuitively understood, because a high value of minimum overlap results in a highly conductive pathway throughout the entire molecule. The importance of π - π overlap to CT has been recognized previously,⁵⁹⁻⁶² although no specific geometrical criterion has been formulated. Note that unlike other parameters, which are independent of each other, the overlap area depends on all other inter base pair parameters with the exception of rise. Therefore, the strong correlation of current with overlap means that while the individual parameters are not important on their own (because, for example, a decrease in shift can be balanced by an increase in slide), their total effect on the base pair stacking is what matters.

The dependence of current on the minimum of overlap areas is plotted in Fig. 1(e). This figure also shows a data point for the ideal B-DNA, with all bases equally spaced, which has

TABLE I. Correlation coefficients between current and inter base pair parameters of 10 poly(G) poly(C) DNA. Overlap areas are calculated between guanines.

	Average	Minimum	Maximum
Twist	0.49	0.15	-0.06
Roll	0.16	-0.01	0.01
Tilt	0.13	0.18	0.20
Rise	-0.08	0.24	0.16
Slide	0.38	0.38	-0.17
Shift	0.46	0.62	0.13
Overlap	0.42	0.91	0.05

a higher minimum overlap area than any of the snapshots. As expected, it carries a much higher current.

This is the first time that a clear correlation with a single structural parameter has been identified. A previous study⁶³ found that the transverse motions of the DNA bases are critical for CT, but did not identify the most relevant structural parameter(s). Another study⁶⁴ concluded that CT can be predicted by internal bond lengths in purine bases. We have considered this criterion, but it did not yield significant correlation with the observed currents. The finding that the minimum of overlaps, rather than their average, controls CT demonstrates its high sensitivity to local conformation. This has important consequences for the biological role of CT, which is hypothesized to be used by the DNA repair enzyme, MutY, to identify areas containing mismatches and lesions.⁶⁵ Our finding provides additional support for this hypothesis.

To understand how surrounding water molecules affect the CT, their number is varied and the results are shown in Fig. 3(a) for configuration 3, the most conductive snapshot of the dry DNA. Clearly, the current decreases with an increasing number of water molecules. The right panel of Fig. 3(a) compares isosurfaces of the most conducting HOMO state for the beginning and end points of the curve. It shows that the increasing screening of phosphate groups in the DNA backbone with an increasing number of solvent molecules suppresses the delocalization of the HOMO state over that region. This eliminates a CT channel through the DNA backbone and decreases the current.

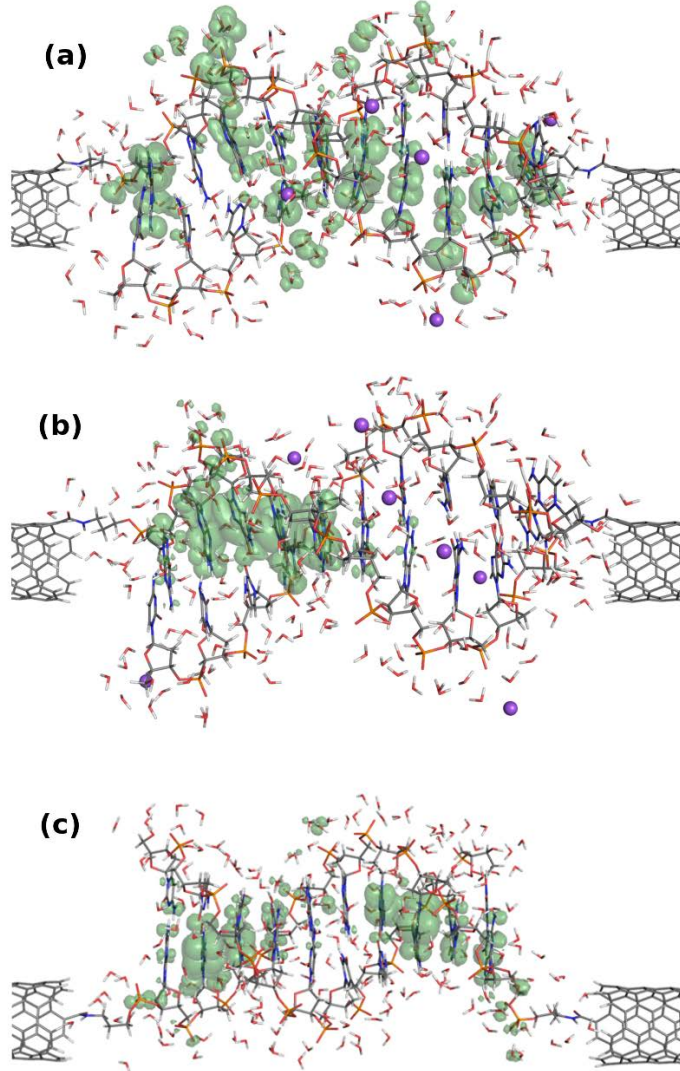


FIG. 2. Isosurfaces of charge densities of the most conducting HOMO states for: (a) a highly and (b) a poorly conducting room temperature conformations of a 10 bp poly(G)-poly(C) DNA. The pink spheres show Na^+ counterions. (c) The same quantity when the 6th base pair is replaced by a GT mismatch. Ions are omitted for clarity in the last case.

Ions in the solvent environment can also reduce the CT by decreasing delocalization of the HOMO states when they are near guanine bases. This is demonstrated in Fig. 3(b) for configuration 3, which contains one such ion near the last guanine from the left, while another ion is nearby a charged phosphate group. When the first ion is removed from the calculation, one of the conductive HOMO states shifts in energy and becomes more delocalized, as shown in the right panel of Fig. 3(b). This causes an approximately three-fold increase in the current. However, the removal of the ion at the phosphate group causes

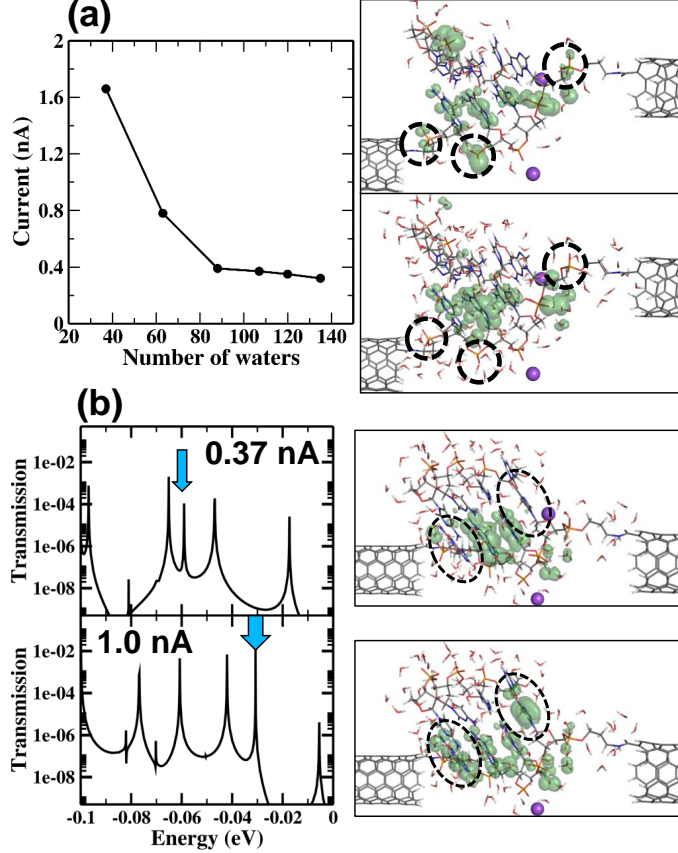


FIG. 3. (a) Current as a function of the number of water molecules closest to the DNA (left panel). The right panel shows the most conductive HOMO state for 37 (top) and 135 (bottom) water molecules. (b) Transmission spectra (left) and partial charge densities (right) for all ions included (top), and when the ion near guanine is removed (bottom).

no significant changes in the current or transmission spectrum.

For comparison, the other homogeneous sequence, poly(A)-poly(T), is also investigated. Here, adenine takes on guanine's role as the main location of conductive HOMO states, but it has a higher ionization potential. This type of DNA is more flexible due to weaker intra-base-pair bonding and also has smaller overlaps between purine bases. Based on these facts, one can expect this sequence to be a worse conductor and this is indeed the case for the ideal B-DNA conformation, where a seven times lower current, 0.0035 nA, is found. However, averaging currents of room temperature conformations yields a value almost exactly the same as for the poly(G)-poly(C) case. The calculated currents are listed in the second column of Table II. An important difference is that for the poly(A)-poly(T) DNA, the minimum of overlap areas, while still being the most relevant structural parameter, is no longer as well

TABLE II. Average currents (nA) for ideal and dynamic DNA structures.

	poly(G)-poly(C)	poly(A)-poly(T)	poly(G)-poly(C) AT mutation	poly(G)-poly(C) GT mutation	poly(G)-poly(C) AC mutation
Ideal	0.0252	0.0035	0.0058	0.0046	0.0048
Dynamic	0.0029	0.0028	0.0021	0.0028	0.0033

correlated with current - its correlation coefficient is only 0.38.

Experiments have shown that even a single mismatched pair can dramatically decrease conductivity.¹³ To examine this, a base pair in the middle of a 10 bp poly(G)-poly(C) DNA is mutated to one of three possibilities: GT, AC and AT. The first two are mismatches, while the third one is well-matched. The results are summarized in the last three columns of Table II.

Comparison with the unperturbed sequence shows that in the ideal B-DNA conformation a mutation to a different base pair causes an approximately a five-fold decrease regardless of the nature of the pair. This is because the substitutions cause a break in the conducting HOMO states located on guanines, as shown in Fig. 2(c). This is consistent with previous first-principles calculations,^{2,42} which found that even a modest sequence variation in the poly(G)-poly(C) sequence limits the coherent transport mechanism. However, for room temperature conformations, each case yields approximately the same average current, which is also comparable to those of the homogeneous sequences. This behavior is consistent with several experimental works,^{23,66,67} which showed that a sequence variation in a homogeneous DNA chain reduces the CT signal at low temperatures, but this effect diminishes as temperature increases.

Coherent CT decays exponentially with length. For DNA, various values of the exponential decay factor have been estimated, ranging from 1.0 to 0.05 \AA^{-1} .^{12,20,23,68-72} Here, we have considered both 4 bp and 10 bp DNA and the obtained average currents can be used to estimate the decay parameter. We find a low value of 0.18 \AA^{-1} , which compares favorably with other molecular wire candidates, for which values between 1 and 0.2 have been reported.^{14,73,74} While previous works^{17,75} have estimated that the coherent CT is relevant only over distances of about 3 bp, but the low value of the decay parameter taken together with extended delocalized regions indicates that coherent transport is relevant over much

longer distances.

IV. SUMMARY AND CONCLUSIONS

Our *ab initio* simulations investigate effects of solvent, conformation and sequence on CT in DNA. The results show that: (i) coherent transport can occur over much longer distances than assumed in the currently accepted DNA CT models, (ii) thermally-induced changes in DNA conformation cause dramatic differences in instantaneous conductivity so that the coherent CT switches between CT active and inactive states; (iii) solvent environment can alter the conductivity by an order of magnitude, but conformational changes are still more important effect. We also find that although mismatched base pairs can lower the conductivity significantly for specific DNA conformations, thermally-induced conformational fluctuations wash out this effect. Nevertheless, the weak dependence of CT on molecular length makes B-DNA a promising candidate for nanoelectronic applications. In particular, immobilizing a partially dried poly(G)-poly(C) B-DNA on a substrate would lead to consistent conductive properties and thus be preferable for applications.

V. ACKNOWLEDGMENTS

BT was supported by AFOSR grant FA9550-13-C-0003, MH and JB by DOE DE-FG02-98ER45685, and WL by ONR N000141010179. Petascale code development was supported by NSF ACI-1339844. The supercomputer time was provided by NSF grant OCI-1036215 at the National Center for Supercomputing Applications and by DOE at the National Center for Computational Sciences at ORNL.

¹ D. D. Eley and D. I. Spivey, "Semiconductivity of organic substances. part 9.—Nucleic acid in the dry state," *Trans. Faraday Soc.* **58**, 411 (1962).

² P. J. de Pablo, F. Moreno-Herrero, J. Colchero, J. Gomez Herrero, P. Herrero, A. M. Baro, P. Ordejon, J. M. Soler, and Emilio Artacho, "Absence of dc-conductivity in λ -DNA," *Phys. Rev. Lett.* **85**, 4992–4995 (2000).

- ³ Y. Zhang, R. H. Austin, J. Kraeft, E. C. Cox, and N. P. Ong, “Insulating behavior of λ -DNA on the micron scale,” *Phys. Rev. Lett.* **89**, 198102 (2002).
- ⁴ D. Porath, A. Bezryadin, S. Vries, and C. Dekker, “Direct measurement of electrical transport through DNA molecules,” *Nature* **403**, 635–638 (2000).
- ⁵ K.-H. Yoo, D. H. Ha, J.-O. Lee, J. W. Park, Jinhee Kim, J. J. Kim, H.-Y. Lee, T. Kawai, and Han Yong Choi, “Electrical conduction through poly(dA)-Poly(dT) and poly(dG)-Poly(dC) DNA molecules,” *Phys. Rev. Lett.* **87**, 198102 (2001).
- ⁶ A. Yu. Kasumov, “Proximity-induced superconductivity in DNA,” *Science* **291**, 280–282 (2001).
- ⁷ R. Endres, “Colloquium: The quest for high-conductance DNA,” *Rev. Mod. Phys.* **76**, 195–214 (2004).
- ⁸ C. J. Murphy, M. R. Arkin, Y. Jenkins, N. D. Ghatlia, S. H. Bossmann, N. J. Turro, and J. K. Barton, “Long-range photoinduced electron transfer through a DNA helix,” *Science* **262**, 1025–1029 (1993).
- ⁹ S. O. Kelley and J. K. Barton, “Electron transfer between bases in double helical DNA,” *Science* **283**, 375–381 (1999).
- ¹⁰ H. Cohen, C. Nogues, R. Naaman, and D. Porath, “Direct measurement of electrical transport through single DNA molecules of complex sequence,” *Proc. Natl. Acad. Sci. U.S.A.* **102**, 11589–11593 (2005).
- ¹¹ J. Hihath, B. Xu, P. Zhang, and N. Tao, “Study of single-nucleotide polymorphisms by means of electrical conductance measurements,” *Proc. Natl. Acad. Sci. U.S.A.* **102**, 16979–16983 (2005).
- ¹² B. Xu, P. Zhang, X. Li, and N. Tao, “Direct conductance measurement of single DNA molecules in aqueous solution,” *Nano Lett.* **4**, 1105–1108 (2004).
- ¹³ X. Guo, A. A. Gorodetsky, J. Hone, J. K. Barton, and bC. Nuckolls, “Conductivity of a single DNA duplex bridging a carbon nanotube gap,” *Nat. Nano* **3**, 163–167 (2008).
- ¹⁴ S. H. Choi, B. Kim, and C. D. Frisbie, “Electrical resistance of long conjugated molecular wires,” *Science* **320**, 1482–1486 (2008).
- ¹⁵ M. E. Núñez, D. B. Hall, and J. K. Barton, “Long-range oxidative damage to dna: effects of distance and sequence,” *Chem. Biol.* **6**, 85–97 (1999).
- ¹⁶ B. Giese, “Long-distance charge transport in DNA: the hopping mechanism,” *Acc. Chem. Res.* **33**, 631–636 (2000).

- ¹⁷ B. Giese, J. Amaudrut, A. Kohler, M. Spormann, and S. Wessely, "Direct observation of hole transfer through DNA by hopping between adenine bases and by tunnelling," *Nature* **412**, 318–320 (2001).
- ¹⁸ E. M. Conwell, "Charge transport in dna in solution: The role of polarons," *Proc. Natl. Acad. Sci. U.S.A.* **102**, 8795–8799 (2005).
- ¹⁹ D. Ly, L. Sani, and G. B. Schuster, "Mechanism of charge transport in dna: internally-linked anthraquinone conjugates support phonon-assisted polaron hopping," *J. Am. Chem. Soc.* **121**, 9400–9410 (1999).
- ²⁰ P. T. Henderson, D. Jones, G. Hampikian, Y. Kan, and G. B. Schuster, "Long-distance charge transport in duplex dna: the phonon-assisted polaron-like hopping mechanism," *Proc. Natl. Acad. Sci. U.S.A.* **96**, 8353–8358 (1999).
- ²¹ E. M. Conwell and S. V. Rakhmanova, "Polarons in dna," *Proc. Natl. Acad. Sci. U.S.A.* **97**, 4556–4560 (2000).
- ²² F. Shao, M. A. O'Neill, and J. K. Barton, "Long-range oxidative damage to cytosines in duplex dna," *Proc. Natl. Acad. Sci. U.S.A.* **101**, 17914–17919 (2004).
- ²³ M. A. O'Neil and J. K. Barton, "DNA charge transport: conformationally gated hopping through stacked domains," *J. Am. Chem. Soc.* **126**, 11471–11483 (2004).
- ²⁴ T. A. Zeidan, R. Carmieli, R. F. Kelley, T. M. Wilson, F. D. Lewis, and M. R. Wasielewski, "Charge-transfer and spin dynamics in dna hairpin conjugates with perylenediimide as a base-pair surrogate," *J. Am. Chem. Soc.* **130**, 13945–13955 (2008).
- ²⁵ F. Shao, K. Augustyn, and J. K. Barton, "Sequence dependence of charge transport through dna domains," *J. Am. Chem. Soc.* **127**, 17445–17452 (2005).
- ²⁶ K. Kobayashi, "Evidence of formation of adenine dimer cation radical in dna: The importance of adenine base stacking," *J. Phys. Chem. B* **114**, 5600–5604 (2010).
- ²⁷ I. Buchvarov, Q. Wang, M. Raytchev, A. Trifonov, and T. Fiebig, "Electronic energy delocalization and dissipation in single-and double-stranded dna," *Proc. Natl. Acad. Sci. U.S.A.* **104**, 4794–4797 (2007).
- ²⁸ V. M. Kucherov, C. D. Kinz-Thompson, and E. M. Conwell, "Polarons in dna oligomers," *J. Phys. Chem. C* **114**, 1663–1666 (2010).
- ²⁹ Y. A. Mantz, F. L. Gervasio, T. Laino, and M. Parrinello, "Solvent effects on charge spatial extent in DNA and implications for transfer," *Phys. Rev. Lett.* **99**, 058104 (2007).

- ³⁰ D. M. Basko and E. M. Conwell, “Effect of solvation on hole motion in DNA,” *Phys. Rev. Lett.* **88**, 098102 (2002).
- ³¹ I. V. Kurnikov, G. S. M. Tong, M. Madrid, and D. N. Beratan, “Hole size and energetics in double helical DNA: competition between quantum delocalization and solvation localization,” *J. Phys. Chem. B* **106**, 7–10 (2002).
- ³² J. C. Genereux, S. M. Wuerth, and J. K. Barton, “Single-step charge transport through DNA over long distances,” *J. Am. Chem. Soc.* **133**, 3863–3868 (2011).
- ³³ N. Renaud, Y. A. Berlin, F. D. Lewis, and M. A. Ratner, “Between superexchange and hopping: An intermediate charge-transfer mechanism in poly(a)-poly(t) DNA hairpins,” *J. Am. Chem. Soc.* **135**, 3953–3963 (2013).
- ³⁴ L. Xiang, J. L. Palma, C. Bruot, V. Mujica, M. A. Ratner, and N. Tao, “Intermediate tunnelling–hopping regime in dna charge transport,” *Nature chemistry* **7**, 221–226 (2015).
- ³⁵ M. A. Young, G. Ravishanker, and D. L. Beveridge, “A 5-nanosecond molecular dynamics trajectory for b-dna: analysis of structure, motions, and solvation,” *Biophys. J.* **73**, 2313–2336 (1997).
- ³⁶ R. N. Barnett, C. L. Cleveland, A. Joy, U. Landman, and G. B. Schuster, “Charge migration in DNA: ion-gated transport,” *Science* **294**, 567–571 (2001).
- ³⁷ A. A. Voityuk, “Charge transfer in dna: Hole charge is confined to a single base pair due to solvation effects,” *J. Chem. Phys.* **122**, 204904 (2005).
- ³⁸ L. Blancafort and A. A. Voityuk, “Casscf/cas-pt2 study of hole transfer in stacked dna nucleobases,” *J. Phys. Chem. A* **110**, 6426–6432 (2006).
- ³⁹ M. A. O’Neill and J. K. Barton, “DNA-Mediated charge transport requires conformational motion of the DNA bases: elimination of charge transport in rigid glasses at 77 k,” *J. Am. Chem. Soc.* **126**, 13234–13235 (2004).
- ⁴⁰ C. D. Pemmaraju, I. Rungger, X. Chen, A. R. Rocha, and S. Sanvito, “Ab initio study of electron transport in dry poly(g)-poly(c) a-DNA strands,” *Phys. Rev. B* **82**, 125426 (2010).
- ⁴¹ Y. Maeda, A. Okamoto, Y. Hoshiya, T. Tsukamoto, Y. Ishikawa, and N. Kurita, “Effect of hydration on electrical conductivity of DNA duplex: Greens function study combined with DFT,” *Comput. Mat. Science* **53**, 314–320 (2012).
- ⁴² S. S. Mallajosyula, J. C. Lin, D. L. Cox, S. K. Pati, and R. R. P. Singh, “Sequence dependent electron transport in wet DNA: ab initio and molecular dynamics studies,” *Phys. Rev. Lett.*

- 101**, 176805 (2008).
- ⁴³ J. Qi, N. Edirisinghe, M. G. Rabbani, and M. P. Anantram, “Unified model for conductance through dna with the landauer-büttiker formalism,” *Physical Review B* **87**, 085404 (2013).
- ⁴⁴ A. K. Mahapatro, K. J. Jeong, G. U. Lee, and D. B. Janes, “Sequence specific electronic conduction through polyion-stabilized double-stranded dna in nanoscale break junctions,” *Nanotechnology* **18**, 195202 (2007).
- ⁴⁵ J. C. Phillips, R. Braun, W. Wang, J. Gumbart, E. Tajkhorshid, E. Villa, C. Chipot, R. D. Skeel, L. Kal, and K. Schulten, “Scalable molecular dynamics with NAMD,” *J. Comput. Chem.* **26**, 1781–1802 (2005), PMC2486339.
- ⁴⁶ S. E. Feller and A. D. MacKerell, “An improved empirical potential energy function for molecular simulations of phospholipids,” *J. Phys. Chem. A* **104**, 7510–7515 (2000).
- ⁴⁷ B. Larade, J. Taylor, H. Mehrez, and H. Guo, “Conductance, i-v curves, and negative differential resistance of carbon atomic wires,” *Physical Review B* **64**, 075420 (2001).
- ⁴⁸ S. Datta, “Linear-response formulation for mesoscopic systems with arbitrary interactions,” *Physical Review B* **46**, 9493 (1992).
- ⁴⁹ M. Brandbyge, J. L. Mozos, P. Ordejon, J. Taylor, and K. Stokbro, “Density-functional method for nonequilibrium electron transport,” *Physical Review B* **65** (2002), 165401 10.1103/PhysRevB.65.165401.
- ⁵⁰ J. L. Fattebert and J. Bernholc, “Towards grid-based $O(n)$ density-functional theory methods: Optimized nonorthogonal orbitals and multigrid acceleration,” *Phys. Rev. B* **62**, 1713–1722 (2000).
- ⁵¹ M. Nardelli, J. L. Fattebert, and J. Bernholc, “ $O(n)$ real-space method for ab initio quantum transport calculations: Application to carbon nanotube-metal contacts,” *Phys. Rev. B* **64**, 245423 (2001).
- ⁵² W. Lu, V. Meunier, and J. Bernholc, “Nonequilibrium quantum transport properties of organic molecules on silicon,” *Phys. Rev. Lett.* **95**, 206805 (2005).
- ⁵³ S. Moore, E. Briggs, M. Hodak, W. Lu, J. Bernholc, and C. Lee, “Scaling the rmg quantum mechanics code,” in *Proceedings of the Extreme Scaling Workshop* (University of Illinois at Urbana-Champaign, 2012) p. 8.
- ⁵⁴ M. Hodak, S. Wang, W. Lu, and J. Bernholc, “Implementation of ultrasoft pseudopotentials in large-scale grid-based electronic structure calculations,” *Phys. Rev. B* **76**, 085108 (2007).

- ⁵⁵ D. Vanderbilt, "Soft self-consistent pseudopotentials in a generalized eigenvalue formalism," *Phys. Rev. B* **41**, 7892–7895 (1990).
- ⁵⁶ J. P. Perdew, K. Burke, and M. Ernzerhof, "Generalized gradient approximation made simple," *Phys. Rev. Lett.* **77**, 3865–3868 (1996).
- ⁵⁷ X. Lu and W. K. Olson, "3DNA: a software package for the analysis, rebuilding and visualization of threedimensional nucleic acid structures," *Nucl. Acids Res.* **31**, 5108–5121 (2003).
- ⁵⁸ W. L. DeLano, *The PyMOL Molecular Graphics System* (2002).
- ⁵⁹ D. B. Hall and J. K. Barton, "Sensitivity of DNA-Mediated electron transfer to the intervening -stack: a probe for the integrity of the DNA base stack," *J. Am. Chem. Soc.* **119**, 5045–5046 (1997).
- ⁶⁰ J. C. Genereux and J. K. Barton, "Mechanisms for DNA charge transport," *Chem. Rev.* **110**, 1642–1662 (2010).
- ⁶¹ S. S. Mallajosyula and S. K. Pati, "Toward DNA conductivity: A theoretical perspective," *J. Phys. Chem. Lett.* **1**, 1881–1894 (2010).
- ⁶² H. Wagenknecht, "Electron transfer processes in DNA: mechanisms, biological relevance and applications in DNA analytics," *Nat. Prod. Rep.* **23**, 973–1006 (2006).
- ⁶³ A. Troisi and G. Orlandi, "Hole migration in DNA: a theoretical analysis of the role of structural fluctuations," *J. Phys. Chem. B* **106**, 2093–2101 (2002).
- ⁶⁴ E. Hatcher, A. Balaeff, S. Keinan, R. Venkatramani, and D. N. Beratan, "PNA versus DNA: effects of structural fluctuations on electronic structure and hole-transport mechanisms," *J. Am. Chem. Soc.* **130**, 11752–11761 (2008).
- ⁶⁵ E. M. Boon, A. L. Livingston, N. H. Chmiel, S. S. David, and J. K. Barton, "DNA-mediated charge transport for DNA repair," *Proc. Natl. Acad. Sci. U.S.A.* **100**, 12543–12547 (2003).
- ⁶⁶ M. A. O'Neill, H. Becker, C. Wan, J. K. Barton, and A. H. Zewail, "Ultrafast dynamics in DNA-Mediated electron transfer: Base gating and the role of temperature," *Angew. Chem.* **115**, 60766080 (2003).
- ⁶⁷ C. H. Wohlgamuth, M. A. McWilliams, and J. D. Slinker, "Temperature dependence of electrochemical DNA charge transport: Influence of a mismatch," *Anal. Chem.* **85**, 1462–1467 (2013).
- ⁶⁸ C. J. Murphy, M. R. Arkin, Y. Jenkins, N. D. Ghatlia, S. H. Bossmann, N. J. Turro, and J. K. Barton, "Long-range photoinduced electron transfer through a DNA helix," *Science* **262**, 1025–1029 (1993), PMID: 7802858.

- ⁶⁹ D. B. Hall, R. E. Holmlin, and J. K. Barton, "Oxidative DNA damage through long-range electron transfer," *Nature* **382**, 731–735 (1996).
- ⁷⁰ J. D. Slinker, N. B. Muren, S. E. Renfrew, and J. K. Barton, "DNA charge transport over 34 nm," *Nat Chem* **3**, 228–233 (2011).
- ⁷¹ B. Elias, F. Shao, and J. K. Barton, "Charge migration along the DNA duplex: hole versus electron transport," *J. Am. Chem. Soc.* **130**, 1152–1153 (2008).
- ⁷² E. Meggers, M. E. Michel-Beyerle, and B. Giese, "Sequence dependent long range hole transport in DNA," *J. Am. Chem. Soc.* **120**, 12950–12955 (1998).
- ⁷³ H. D. Sikes, J. F. Smalley, S. P. Dudek, A. R. Cook, M. D. Newton, C. E. D. Chidsey, and S. W. Feldberg, "Rapid electron tunneling through oligophenylenevinylene bridges," *Science* **291**, 1519–1523 (2001).
- ⁷⁴ A. Salomon, D. Cahen, S. Lindsay, J. Tomfohr, V. B. Engelkes, and C. D. Frisbie, "Comparison of electronic transport measurements on organic molecules," *Adv. Mater.* **15**, 1881–1890 (2003).
- ⁷⁵ M. Bixon and J. Jortner, "Charge transport in DNA via thermally induced hopping," *J. Am. Chem. Soc.* **123**, 12556–12567 (2001).